Regular Article

Highlighted Paper selected by Editor-in-Chief

Carotenoid Stereochemistry Affects Antioxidative Activity of Liposomes Co-encapsulating Astaxanthin and Tocotrienol

Misuzu Ishikawa,[a,#] Shota Hirai,[a,#] Tatsusada Yoshida,[a] Natsumi Shibuya,[a] Susumu Hama,[b] Yu Takahashi,[c] Tatsuya Fukuta,[a] Tamotsu Tanaka,[a] Shinzo Hosoi,[b] and Kentaro Kogure*[,a]

[a] *Graduate School of Biomedical Sciences, Tokushima University; 1 Shomachi, Tokushima 770–8505, Japan:* [b] *Kyoto Pharmaceutical University; 5 Misasagi-Nakauchicho, Yamashina-ku, Kyoto 607–8414, Japan: and* [c] *Fuji Chemical Industries, Co., Ltd.; 55 Yokohoonji, Kamiichi-machi, Nakaniikawa-gun, Toyama 930–0397, Japan.*

Received January 17, 2018; accepted April 27, 2018

We previously found that antioxidative activity of liposomes co-encapsulating astaxanthin (Asx) and tocotrienols (T3s) was higher than the calculated additive activity, which results from intermolecular interactions between both antioxidants (*J. Clin. Biochem. Nutr.*, 59, 2016, Kamezaki *et al.*). Herein, we conducted experiments to optimize Asx/α-T3 ratio for high antioxidative activity, and tried to elucidate details of intermolecular interaction of Asx with α-T3. Higher activity than calculated additive value was clearly observed at an Asx/α-T3 ratio of 2 : 1, despite two α-T3 would potentially interact with two terminal rings of one Asx. The synthetic Asx used in this study was a mixture of three stereoisomers, 3*R*,3′*R*-form (Asx-*R*), 3*S*,3′*S*-form (Asx-*S*) and 3*R*,3′*S*-*meso* form (Asx-*meso*). The calculated binding energy of the Asx-*S*/α-T3 complex was higher than those of Asx-*R*/α-T3 and Asx-*meso*/α-T3, suggesting that Asx-*S* and α-T3 is the most preferable combination for the intermolecular interaction. The optimal Asx-*S*/α-T3 ratio for antioxidation was shown to be 1 : 2. These results suggest that the Asx stereochemistry affects the intermolecular interaction of Asx/α-T3. Moreover, the absorption spectrum changes of Asx-*S* upon co-encapsulation with α-T3 in liposomes indicate that the electronic state of Asx-*S* is affected by intermolecular interactions with α-T3. Further, intermolecular interactions with α-T3 affected the electronic charges on the C9, C10 and C15 atoms in the polyene moiety of Asx-*S*. In conclusion, the intermolecular interaction of Asx/T3 depends on the Asx stereochemistry, and caused a change in the electronic state of the Asx polyene moiety by the presence of double bond in the T3 triene moiety.

Key words antioxidation; astaxanthin stereoisomer; tocotrienol; intermolecular interaction

Astaxanthin (Asx, 3,3′-dihydroxy-β,β-carotene-4,4′-dione; Fig. 1) is a carotenoid, and is known as a hydrophobic red pigment found in algae, fish, and birds.[1,2] Asx is a more potent antioxidant than the representative carotenoid, β-carotene, for removal of reactive oxygen species (ROS), especially singlet oxygen.[3] We previously reported that Asx prevented lipid peroxidation in various biological membranes, such as phosphatidylcholine liposomes and rat liver mitochondria.[4–8] We suggested that the potent antioxidative activity of Asx in biological membranes is attributable to the polyene moiety and terminal ring moieties of Asx, which react with free radicals at the interface and hydrophobic region of lipid membranes, respectively.[7] As Asx is a highly hydrophobic compound, we prepared liposomes encapsulating Asx (Asx-lipo) in phospholipid membranes to evaluate the antioxidative activity in aqueous assay systems. We recently found that Asx can scavenge hydroxyl radicals,[9] suggesting that Asx-lipo was able to have potent antioxidative effects against various ROS. In addition, we demonstrated that UV-induced melanin production in the skin was able to be prevented by transdermal delivery of Asx-lipo *via* iontophoresis.[10] This anti-melanin production effect of Asx-lipo would be due to the potent radical scavenging capacity of Asx in lipid membranes.

To improve the antioxidative capacity of Asx-lipo, we investigated the additive effect of other antioxidative compounds, such as vitamin E. Specifically, we previously evaluated the *in vitro* antioxidative activity of liposomes co-encapsulating Asx and vitamin E derivatives, α-tocopherol (α-T) and tocotrienols (T3), against singlet oxygen and hydroxyl radical.[11] The antioxidative activity of liposomes co-encapsulating Asx and α-T was lower than the sum of the scavenging activities of Asx-lipo and liposomes encapsulating α-T. On the other hand, the antioxidative activity of liposomes co-encapsulating Asx and T3 was higher than the calculated additive activity. Calculation of the most stable molecular structure of Asx in the presence of α-T or α-T3 suggested that only α-T3 was predicted to form hydrogen bonding with Asx, and that the Asx polyene chain partially interacts with the α-T3 triene chain[11] (Fig. 1). These results suggested that intermolecular interactions would be responsible for the increased antioxidative activity of liposomes co-encapsulating Asx and α-T3. To elucidate the details of the intermolecular interaction of Asx with α-T3, further investigations are needed to provide stoichiometric information, and to better understand the mechanism of the increased antioxidative activity of liposomes co-encapsulating Asx and α-T3.

In the present study, we determined the optimal Asx/α-T3 ratio needed for higher antioxidative activity of the co-encapsulated liposomes than calculated additive activity, to identify the stoichiometry required for favorable intermolecular interactions between Asx and α-T3. Moreover, as Asx has three stereochemical isomers, the effect of stereochemistry on the optimal ratio was also examined. In addition, the effect of intermolecular interactions between Asx and α-T3 on the reactivity of Asx was investigated using computational methods.

[#] These authors contributed equally to this work.

* To whom correspondence should be addressed. e-mail: kogure@tokushima-u.ac.jp

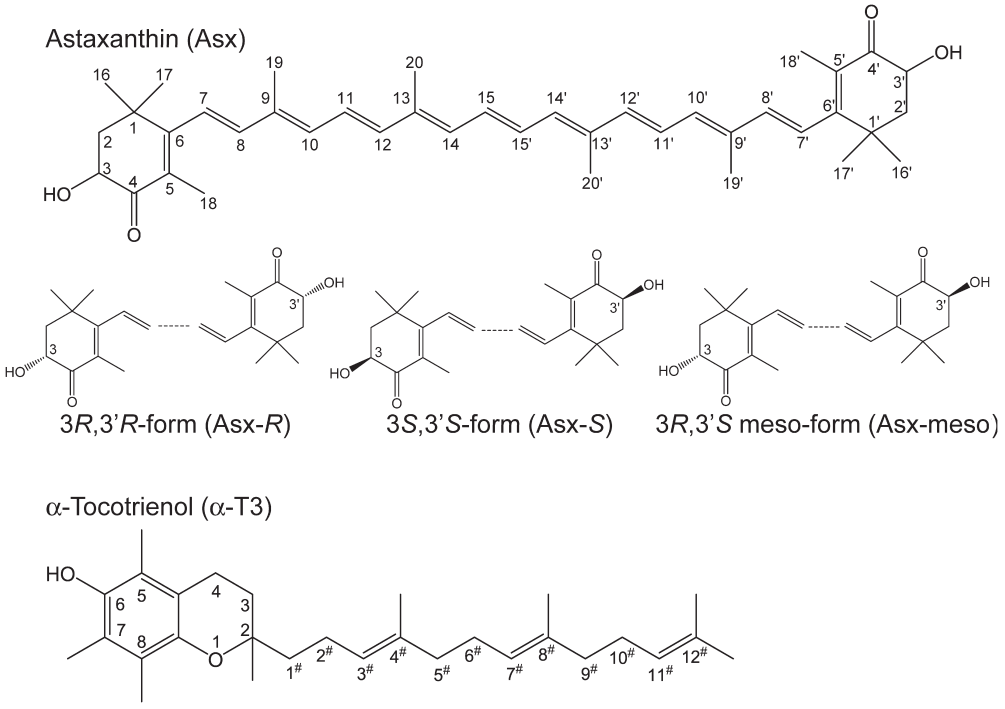

Fig. 1. Chemical Structures of Astaxanthin (Asx), Asx Stereoisomers 3*R*,3′*R*-Form (Asx-*R*), 3*S*,3′*S*-Form (Asx-*S*) and 3*R*,3′*S*-*meso* Form (Asx-*meso*) and *α*-Tocotrienol (*α*-T3)

Experimental

Materials Synthetic Asx and *α*-T3 were purchased from Sigma-Aldrich Co., LLC. (U.S.A.). 3*S*,3′*S*-Form Asx (Asx-*S*) was manufactured by Fuji Chemical Industries Co., Ltd. (Japan). Egg phosphatidylcholine (EPC) was obtained from the NOF Corporation (Tokyo, Japan). Aminophenyl fluorescein (APF) was purchased from Goryo Chemical, Inc. (Sapporo, Japan). All other reagents were of the highest commercially available grade.

Preparation of Liposomes Encapsulating Asx and *α*-T3 EPC liposomes encapsulating Asx and *α*-T3 were prepared using a lipid hydration method.[12] Chloroform solutions containing 2 μmol EPC, Asx and *α*-T3, were dried to obtain a thin lipid film under vacuum in a glass tube. The dried lipid film was hydrated with 0.2 mL 10 mM Tris buffer (pH 7.4) at room temperature, and liposomes were produced by sonication of the hydrated lipid film in a bath-type sonicator (AU-25C, Aiwa, Tokyo, Japan). The sizes of the liposomes encapsulating the antioxidants were measured by dynamic light scattering using a Zetasizer nano (Malvern Instruments Ltd., U.K.). The diameters of the liposomes were summarized in Table 1.

Evaluation of Hydroxyl Radical Scavenging Activity of Liposomes Hydroxyl radical production was evaluated by measuring the fluorescence intensity of APF.[13] Hydroxyl radicals are known to be generated by the Fenton reaction as follows: $Fe^{2+}+H_2O_2 \rightarrow Fe^{3+}+OH^-+\cdot OH$.[14] To generate hydroxyl radicals, 30 μL of 10 mM H_2O_2 (final concentration: 1 mM), 45 μL of a 10 mM liposomal suspension (final lipid concentration: 1.5 mM), 30 μL of a 100 μM APF solution (final concentration: 10 μM), and 30 μL of a 1 mM $FeSO_4$ solution (final concentration: 100 μM) were mixed in a test tube. After mixing, the fluorescence intensity (excitation: 490 nm; emission: 515 nm) was measured within 10 s by a microplate reader Infinite M200 (Tecan Group Ltd., Switzerland).

Table 1. Diameters of Liposomes Used in This Study

Liposomes	Diameter (nm)
Control	292.5±97.1
α-T3-lipo (*α*-T3 7.5 μM)	260.5±67.5
Asx-lipo (Asx 1.875 μM)	280.6±76.2
Asx-lipo (Asx 3.75 μM)	262.3±56.3
Asx-lipo (Asx 7.5 μM)	270.9±62.0
Asx-lipo (Asx 15 μM)	253.7±63.4
Asx-lipo (Asx 30 μM)	297.9±90.7
Asx/*α*-T3-lipo (Asx 1.875 μM/*α*-T3 7.5 μM)	242.6±39.3
Asx/*α*-T3-lipo (Asx 3.75 μM/*α*-T3 7.5 μM)	303.1±59.5
Asx/*α*-T3-lipo (Asx 7.5 μM/*α*-T3 7.5 μM)	284.7±95.0
Asx/*α*-T3-lipo (Asx 15 μM/*α*-T3 7.5 μM)	257.2±46.9
Asx/*α*-T3-lipo (Asx 30 μM/*α*-T3 7.5 μM)	271.6±76.4
Asx-*S*-lipo (Asx-*S* 1.875 μM)	250.2±107.5
Asx-*S*-lipo (Asx-*S* 3.75 μM)	290.4±165.0
Asx-*S*-lipo (Asx-*S* 7.5 μM)	232.9±141.6
Asx-*S*-lipo (Asx-*S* 15 μM)	231.0±78.4
Asx-*S*-lipo (Asx-*S* 30 μM)	245.5±116.8
Asx-*S*/*α*-T3-lipo (Asx-*S* 1.875 μM/*α*-T3 7.5 μM)	276.3±147.4
Asx-*S*/*α*-T3-lipo (Asx-*S* 3.75 μM/*α*-T3 7.5 μM)	237.7±141.0
Asx-*S*/*α*-T3-lipo (Asx-*S* 7.5 μM/*α*-T3 7.5 μM)	266.5±140.1
Asx-*S*/*α*-T3-lipo (Asx-*S* 15 μM/*α*-T3 7.5 μM)	290.2±115.3
Asx-*S*/*α*-T3-lipo (Asx-*S* 30 μM/*α*-T3 7.5 μM)	244.1±85.3

Concentration value in parentheses of each liposome corresponds to the concentration of each antioxidant used in Figs. 2 and 5. The values are averages±S.D. of at least three samples prepared at different days.

Estimation of Hydroxyl Radical-Mediated Cytotoxicity Swiss 3T3 cells were cultured (1×10^5 cells/well of 24-well plate) in Dulbecco's modified Eagle's medium (DMEM) containing 10% fetal bovine serum (FBS) at 37°C in a 5% CO_2 atmosphere for 24 h. The medium was then removed, and DMEM containing 1 mM of liposomes was added to the cells.

The cells were incubated with the medium containing liposomes for 30 min at 37°C. After incubation, the medium was removed, and the cells were incubated with DMEM containing 10 mM $FeSO_4$ and 10 mM H_2O_2 at 37°C for 30 min. After incubation, DMEM was removed, and the cells were collected by treatment with trypsin. The collected cells were stained with 0.4% trypan blue, and the numbers of total cells and stained cells were counted.

Estimation of the Intermolecular Interaction Energy and Distance between the Polyene Chain of Asx and the Triene Chain of α-T3 All calculations were performed using the technical computing software SCIGRESS Ver. 2.1.0 (build 3050; Fujitsu Co., Ltd., Chiba, Japan). The minimum energy conformations of the Asx stereoisomers, 3*R*,3′*R*-form (Asx-*R*), 3*S*,3′*S*-form (Asx-*S*), and 3*R*,3′*S*-form (Asx-*meso*), with α-T3, were first calculated using molecular mechanics (CONFLEX-MM3). Starting from the calculated conformations, optimized structures were then predicted using semi-empirical molecular calculations (PM6). The intermolecular interaction energies were estimated by the heat of formation difference for each of the following combinations calculated using PM6: Asx-*R*–α-T3, Asx-*S*–α-T3, and Asx-*meso*–α-T3. Intermolecular distances were determined using the optimized complex structures.

Visible Absorption Spectrum of Liposomes Encapsulating Asx-*S* and α-T3 Visible absorption spectra (400–600 nm) of suspensions containing liposomes encapsulating Asx-*S* (Asx-*S*-lipo), liposomes encapsulating α-T3 (α-T3-lipo), and liposomes co-encapsulating Asx-*S* and α-T3 (Asx-*S*/α-T3-lipo), of which molar ratio of Asx-*S*/α-T3 was 1 : 2, were measured with a NanoPhotometer C40 (Implen GmbH, Germany). The concentration of each liposomal suspension was the same as described above. The absorption spectrum of EPC liposomes without Asx-*S* and α-T3 was subtracted from the absorption spectrum of liposomes encapsulating each of the antioxidant, to cancel liposomal turbidity.

Prediction of Effect of Intermolecular Interactions with α-T3 on the Electronic Structure of Asx-*S* All electronic structure calculations were carried out with the Gaussian 09 program.[15] The B3LYP-D3(BJ) hybrid density functional theory (DFT) functional, which contains Grimme's empirical dispersion correction (D3(BJ)) term[16] was used. The initial structure of the Asx-*S*/α-T3 complex was prepared based on our previously reported method.[11] The geometry of the complex, as well as that of Asx-*S* alone, was then fully optimized using the 6-31G(d) basis set. The zero-point energy (ZPE) corrected homolytic C–H bond dissociation energy (BDE) was calculated at the B3LYP-D3(BJ)/6-311+G(d,p)//B3LYP-D3(BJ)/6-31G(d) level for Asx-*S*, both alone and in the Asx-*S*/α-T3 complex. To examine a change in charge distribution within Asx-*S* due to complex formation with α-T3, Δq_i(Asx-*S*) (=q_i(Asx-*S*)complex−q_i(Asx-*S*)alone), we performed natural population analysis[17] at the same level. q_i(Asx-*S*)complex and q_i(Asx-*S*)alone denote the natural charge on the *i*-th atom within Asx-*S* in the complex state and alone, respectively. The contribution of hydrogen atoms to Δq_i(Asx-*S*) was summed into the heavy atoms.

Statistical Analysis Statistical analysis was performed using one-way ANOVA followed by the Turkey–Kramer honest significant difference (HSD) test. p values <0.05 were considered to be significant, and were evaluated using Kaleida Graph (HULINKS Inc., Japan).

Results and Discussion

To optimize the Asx/α-T3 ratio for higher scavenging activity than additive activity of each single antioxidant against hydroxyl radicals, we measured the hydroxyl radical scavenging activity of liposomes co-encapsulating various Asx/α-T3 ratios. The hydroxyl radical scavenging activity was augmented with increasing amount of Asx (Fig. 2). Only at an Asx/α-T3 ratio of 2 : 1, the hydroxyl radical scavenging activity of Asx/α-T3-lipo was higher than the sum of the activities of Asx-lipo and α-T3-lipo. At other ratios investigated, the activity of Asx/α-T3-lipo was nearly the same as the combined activities of Asx-lipo and α-T3-lipos.

To confirm the usefulness of Asx/α-T3-lipo as antioxidative nanoparticles, we evaluated the protective effects of Asx/α-T3-lipo at various Asx/α-T3 ratios on hydroxyl radical-mediated cytotoxicity (Fig. 3). Although both Asx-lipo and α-T3-lipo demonstrated protective effects against hydroxyl radical-mediated cytotoxicity, the effects were not so potent. In our experimental condition, no protective effect on cytotoxicity was observed at less than 5 μM of Asx. Thus, the effect of Asx-lipo was examined at the higher concentration than 5 μM.

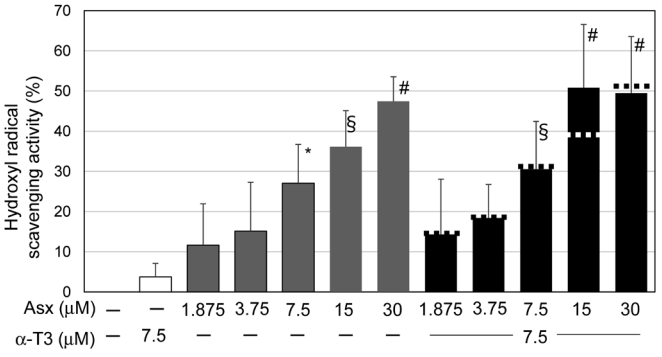

Fig. 2. Effect of Co-encapsulation of Asx and α-T3 in Liposomes on Hydroxyl Radical Scavenging

Relative hydroxyl radical scavenging activities of liposomes containing α-T3 (white column), Asx (gray column), and both Asx and α-T3 (black column) were evaluated by the decrease in fluorescence intensity of APF due to hydroxyl radical production. The combined values of liposomes encapsulating either Asx or α-T3 alone are denoted by dotted lines. Data are means±S.D. determined from separate measurements ($n>3$). Statistical significance at $p<0.05$; # *vs.* control, 7.5 μM α-T3, 1.875 μM Asx, 3.75 μM Asx, 7.5 μM α-T3+1.875 μM Asx, and 7.5 μM α-T3+3.75 μM Asx; § *vs.* control and 7.5 μM α-T3; * *vs.* control.

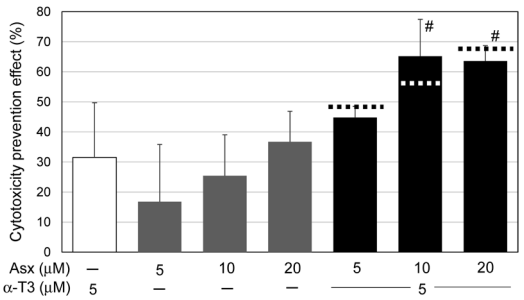

Fig. 3. Effect of Liposomes Co-encapsulating Asx and α-T3 on the Viability of Cells Treated with Fenton's Reagent

H_2O_2 and $FeSO_4$ solution were added to Swiss 3T3 cells after incubation with the liposome suspension. Cell viability was evaluated by staining with trypan blue. The combined values of liposomes encapsulating either Asx or α-T3 alone are denoted by dotted lines. Data are means±S.D. determined from separate measurements ($n>3$). Statistical significance at $p<0.05$; # *vs.* 5 μM Asx and 10 μM Asx.

On the other hand, the protective effect of Asx/α-T3-lipo was higher than that of both Asx-lipo and α-T3-lipo. The protective effects observed at Asx/α-T3 ratios of 1 : 1 and 4 : 1 were slightly lower than the sum of liposomes containing single antioxidants (Asx-lipo and α-T3-lipo), while Asx/α-T3-lipo prepared at a ratio of 2 : 1 demonstrated more potent effects than the sum of Asx-lipo and α-T3-lipo (Fig. 3), suggesting that prevention of hydroxyl radical-mediated cytotoxicity was due to a synergistic effect associated with a combination of both antioxidants at an Asx/α-T3 ratio of 2 : 1. Thus, Asx/α-T3-lipo, which exhibits higher antioxidative activity than additive activity, would be useful as nanoparticles for the prevention of cellular damage induced by ROS.

Based on the observed higher antioxidative activity of Asx/α-T3-lipo than additive activity of each single antioxidant liposome, the optimal Asx/α-T3 ratio was determined to be 2 : 1. However, it was previously suggested that both the hydroxyl group and the carbonyl group of Asx make hydrogen bonding with the phenolic hydroxyl group of α-T3.[11] Since Asx has two terminal ring moieties (Fig. 1), it would be possible for a single Asx molecule to interact with two α-T3 molecules. Thus, the identified optimal Asx/α-T3 ratio (2 : 1) is inconsistent with the predicted stoichiometry (*i.e.*, Asx/α-T3=1 : 2). It is known that Asx have three stereoisomers, namely 3*R*,3′*R*-form (Asx-*R*), 3*S*,3′*S*-form (Asx-*S*) and 3*R*,3′*S*-*meso* form (Asx-*meso*)[18] (Fig. 1). The synthetic Asx used in the optimization experiment was a mixture of 3 stereoisomers, namely Asx-*R*, Asx-*S* and Asx-*meso*, of which the composition ratio should be 1 : 1 : 2.[18] As the directions of the OH groups of the terminal ring moieties are different in the different stereoisomers, it was expected that the stereochemistry of Asx might affect the intermolecular interactions with α-T3. To investigate the effect of Asx stereochemistry on intermolecular interactions between Asx and α-T3, estimations of the intermolecular interaction energies of the Asx stereoisomers with α-T3 were performed using semi-empirical molecular orbital calculations (PM6). The heats of formation of Asx-*R*, Asx-*S* and Asx-*meso* with α-T3 were determined to be 8.7, 9.7 and 7.9 kcal/mol, respectively (Fig. 4). Based on these results, it was suggested that Asx-*S* exhibits the most potent intermolecular interaction with α-T3, and that a molecular complex of Asx-*S* with α-T3 in liposomal membranes is preferable over combinations containing either Asx-*R* or Asx-*meso*.

To confirm the stereochemical effect of Asx on the antioxidative activity, the hydroxyl radical scavenging activities of liposomes co-encapsulating various Asx-*S*/α-T3 ratios were measured (Fig. 5). The higher scavenging activity than additive activity of each single antioxidant liposome was observed at low Asx-*S* concentrations (<7.5 μM). Thus, the increased antioxidative activity was clearly observed at an Asx-*S*/α-T3 ratio of 1 : 2 (Fig. 5), in contrast to the optimal ratio identified for the combination of the Asx stereoisomer mixture and α-T3 (*i.e.*, 2 : 1), as mentioned above (Fig. 2). The optimal ratio of Asx-*S*/α-T3 in liposomes was found to be 1 : 2 (Fig. 5), suggesting that the stereochemistry of carotenoids is an important factor for the antioxidative activity of liposomes co-encapsulating Asx and α-T3. The molar ratio of the stereoisomers Asx-*R*, Asx-*S* and Asx-*meso* in synthetic Asx, is known to be 1 : 1 : 2.[18] Thus, the relative molar ratio of Asx-*S* in 1 mol of a mixture of Asx isomers would be 0.25. Based on this estimation, the relative amount of Asx-*S* in liposomes encapsulating Asx/T3 (2 : 1) would be 0.5. Therefore, in the liposomes encapsulating the Asx isomer mixture and α-T3, it was suggested that the relative molar ratio of Asx-*S*/α-T3 was 1 : 2. This estimation is consistent with the results in Fig. 5. However, there is a possibility of interaction of Asx-*R* or Asx-*meso* with α-T3, although binding association coefficient of Asx-*S* was the highest in the three isomers. Since the intermolecular interaction between Asx-*S* and α-T3 would be dynamic, free Asx-*S* and α-T3 would exist in the lipid membrane even in the presence of Asx-*S*/α-T3 complex. Thus, in the case of mixture of Asx isomers, some part of Asx-*R* or Asx-*meso* have a possibility to interact with free α-T3, although the binding association coefficients of Asx-*R*/α-T3 and Asx-*meso*/α-T3 are lower than that of Asx-*S*/α-T3.

To confirm the intermolecular interactions between Asx-*S*

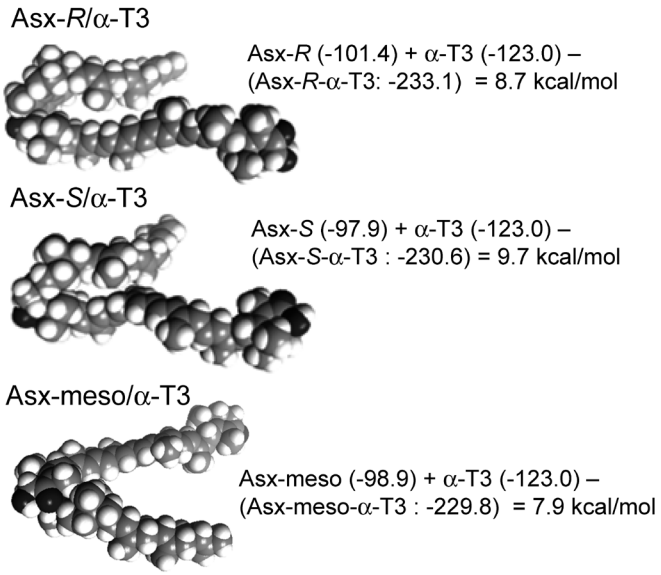

Fig. 4. Comparison of Intermolecular Interaction Energies of Asx Stereoisomers with α-T3

Intermolecular interaction energies of Asx stereoisomers with α-T3 were estimated by semi-empirical molecular orbital calculation (PM6).

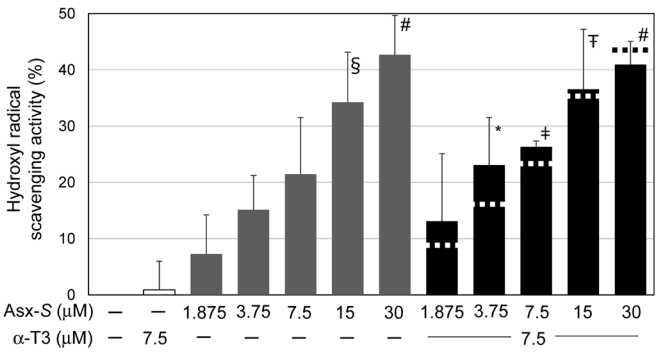

Fig. 5. Effect of Co-encapsulation of Asx-*S* and α-T3 in Liposomes on Hydroxyl Radical Scavenging

Relative hydroxyl radical scavenging activities of liposomes containing α-T3 (white column), Asx-*S* (gray column), or both Asx-*S* and α-T3 (black column) were evaluated by the decrease in fluorescence intensity of APF due to hydroxyl radical production. The combined values of liposomes encapsulating either Asx-*S* or α-T3 alone are denoted by dotted lines. Data are means±S.D. determined from separate measurements ($n>3$). Statistical significance at $p<0.05$; $^{\#}$*vs.* control, 7.5 μM α-T3, 1.875 μM Asx-*S*, 3.75 μM Asx-*S*, and 7.5 μM α-T3+1.875 μM Asx-*S*; §*vs.* control, 7.5 μM α-T3, and 1.875 μM Asx-*S*; $^{\mp}$*vs.* control, 7.5 μM α-T3, 1.875 μM Asx-*S*, and 7.5 μM α-T3+1.875 μM Asx-*S*; †*vs.* control, and 7.5 μM α-T3; **vs.* control.

and α-T3, the visible absorption spectrum of Asx-*S*/α-T3-lipo prepared at the optimal ratio of 1 : 2 was compared with the combined visible absorption spectra of Asx-*S*-lipo and α-T3-lipo (Fig. 6). The visible absorption spectrum of liposomes without Asx-*S* and α-T3 was subtracted from each visible absorption spectrum of liposomes encapsulating antioxidants to cancel liposomal turbidity. The Asx-*S*/α-T3-lipo visible absorption spectrum, which is dominated by Asx-*S*, was different from the combined visible absorption spectra of Asx-*S*-lipo and α-T3-lipo, with the visible absorption peak being slightly shifted to longer wavelengths upon co-encapsulation. Based on these results, it is suggested that the electronic state of Asx-*S* is affected by intermolecular interactions with α-T3.

We previously reported that the hydrogen atoms at C3/C3′ in the terminal ring moieties of Asx was also able to be extracted by a free radical for scavenging ROS.[7] Thus, we expected that the reactivity of the Asx terminal ring moieties would increase *via* intermolecular interactions. To confirm this, reactivity at the terminal ring moieties of Asx-*S* was estimated by calculating the bond dissociation energy (BDE) between C3 and H. The H–C3 BDE of Asx-*S* alone was 71.3

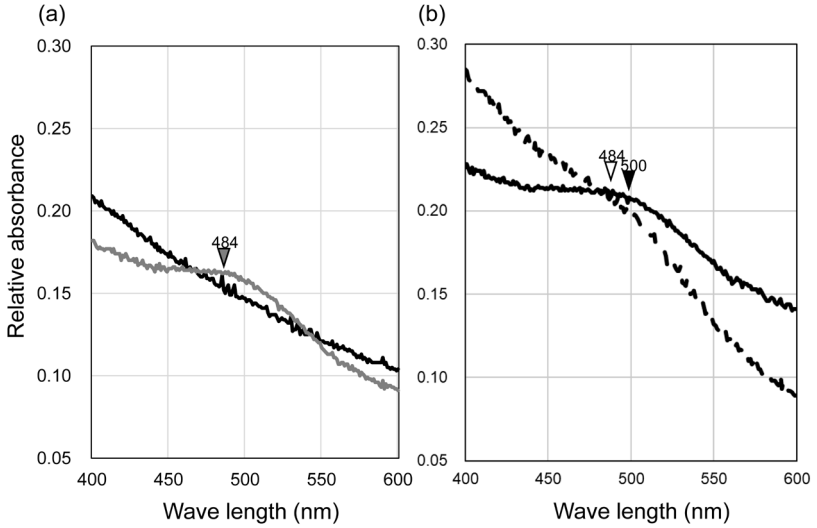

Fig. 6. Visible Absorption Spectra of Liposomes Co-encapsulating of Asx-*S* and α-T3

(a) The visible absorption spectrum of each Asx-*S*-lipo (gray solid line) and α-T3-lipo (black solid line). (b) The visible absorption spectrum of liposomes co-encapsulating Asx-*S* and α-T3 (solid line) was compared with that of a suspension containing Asx-*S*-lipo and α-T3-lipo (dotted line). The peak tops of visible absorption spectra of Asx-*S*-lipo, Asx-*S*/α-T3-lipo and a suspension containing Asx-*S*-lipo and α-T3-lipo were indicated by a gray arrow, a black arrow and a white arrow, respectively.

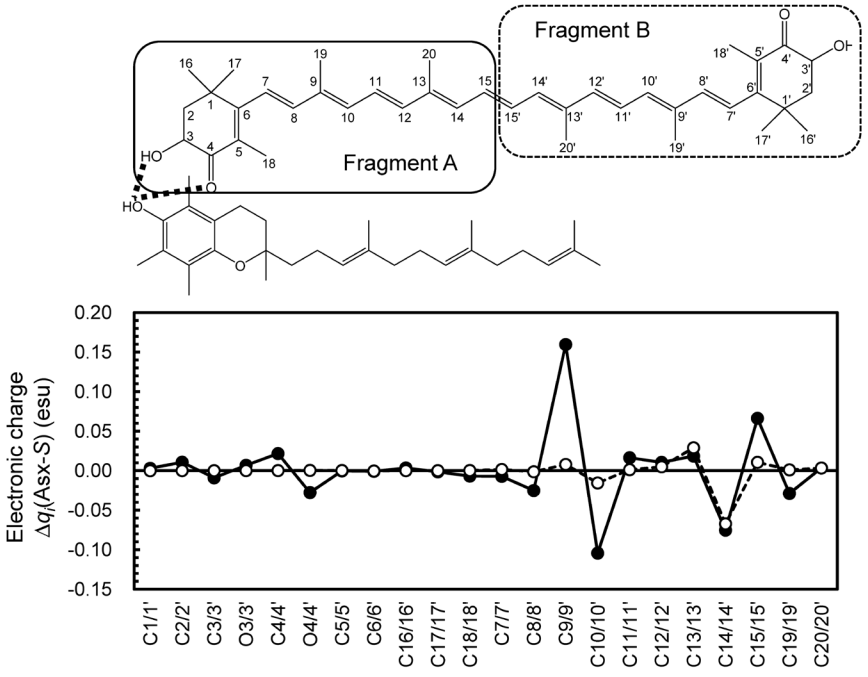

Fig. 7. Effect of Intermolecular Interaction with α-T3 on the Electronic Structure of Asx-*S*

The electronic structure of Asx-*S* half fragment A complexed with α-T3 was compared with free Asx-*S* half fragment B. Δq_i(Asx-*S*) of Asx-*S* half fragment A complexed with α-T3 (closed circle, solid line) and free Asx-*S* half fragment B (open circle, dotted line) were compared.

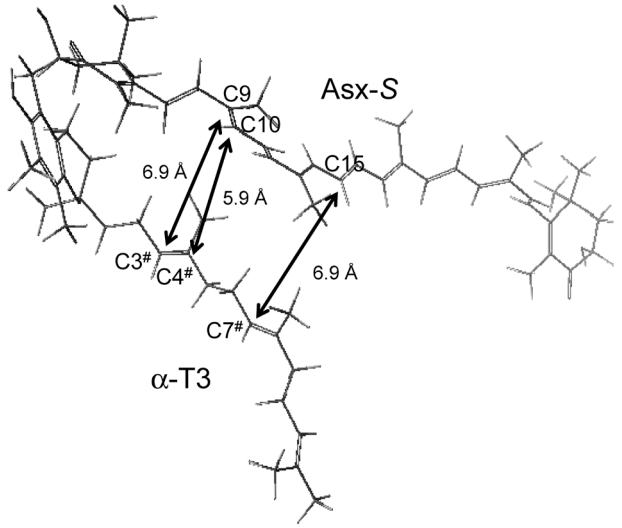

Fig. 8. Intermolecular Distances between C9, C10 and C15 in the Polyene Chain of Asx-*S* and C3#, C4# and C7# in the Triene Chain of *α*-T3

Distances were calculated based on the optimized complex structures, as described in Experimental.

kcal/mol, while the H–C3 BDE of the Asx-*S*/*α*-T3 complex was 71.0 kcal/mol. Contrary to expectation, there was no significant difference in the H–C3 BDEs between Asx-*S* alone and the Asx-*S*/*α*-T3 complex. This result indicates that the reactivities of the terminal ring moieties of Asx-*S* were not changed by intermolecular interaction with *α*-T3. Additionally, the BDEs of the phenolic O–H of *α*-T3 with or without hydrogen bonding with Asx-*S* were calculated. The phenolic O–H BDE of *α*-T3 alone was 71.4 kcal/mol, while the phenolic O–H BDE of the Asx-*S*/*α*-T3 complex was 73.6 kcal/mol. Since the phenolic O–H BDE of *α*-T3 slightly increased by hydrogen bonding with Asx-*S*, it was suggested that the hydrogen bonding between Asx and *α*-T3 might induce any effect on the extraction of H atom from phenolic OH of *α*-T3 by ROS.

It is well known that Asx can also scavenge free radicals *via* the polyene chain, in addition to the terminal ring moieties.[7] Therefore, we evaluated the effect of intermolecular interaction with *α*-T3 on the electronic structure of Asx-*S*. The electronic structure of the Asx-*S* half fragment A, which was complexed with *α*-T3, was compared with that of free Asx-*S* half fragment B (Fig. 7). Interestingly, electronic charges on the C9, C10 and C15 atoms in Asx-*S* were changed by intermolecular interactions with *α*-T3, while the electronic charges on the C3 and H atoms in Asx-*S* half fragment A complexed with *α*-T3 were nearly the same as that of Asx-*S* half fragment B (Fig. 7). The result of visible absorption spectrum (Fig. 6) supports the estimation of the effect of intermolecular interactions with *α*-T3 on the electronic charge of Asx-*S*.

For effective intermolecular interactions, the polyene moiety of Asx should be in close proximity to the triene moiety of *α*-T3. We calculated the distances between C9, C10 and C15 in the polyene chain of the three Asx isomers and C3#, C4# and C7# at the double bond positions in the triene chain of *α*-T3 (Fig. 8). The distances of C9 (Asx-*S*)-C3# (*α*-T3), C10 (Asx-*S*)-C4# (*α*-T3) and C15 (Asx-*S*)-C7# (*α*-T3) were 6.9, 5.9 and 6.9 Å, respectively. These distances were smaller than those of Asx-*R*/*α*-T3 and Asx-*meso*/*α*-T3 (Table 2). It is suggested that a change in the electronic state of the polyene moiety of

Table 2. Distances between C9, C10 and C15 in the Polyene Chain of Asx Isomers and C3#, C4# and C7# in the Triene Chain of *α*-T3

Asx	C9 (Asx)-C3# (*α*-T3)	C10 (Asx)-C4# (*α*-T3)	C15 (Asx)-C7# (*α*-T3)
Asx-*R*	8.0 Å	6.5 Å	7.9 Å
Asx-*S*	6.9 Å	5.9 Å	6.9 Å
Asx-*meso*	9.7 Å	9.9 Å	11.0 Å

Distances were calculated based on the optimized complex structures, as described in Experimental.

Asx-*S* by intermolecular interactions would be responsible for the increased antioxidative activity of liposomes co-encapsulating Asx and *α*-T3. In our previous report, the antioxidative activity of liposomes co-encapsulating Asx with T3, but not tocopherol, was higher than additive activity of each single antioxidant liposome.[11] From the results in Figs. 7 and 8, it is suggested that the alkyl chain of tocopherol could not interact with the polyene chain of Asx, because tocopherol's hydrophobic chain does not contain a double bond. In this study, we could not compare Asx-*R* and Asx-*meso* with Asx-*S*, because pure Asx-*R* and Asx-*meso* were commercially unavailable. In the future, if we obtain Asx-*R* and Asx-*meso*, we would like to compare the antioxidative ability and cytotoxicity prevention effect of those stereoisomers of Asx.

On the other hand, the possibility of the effect of hydrogen bonding between Asx and *α*-T3 on the extraction of H atom from phenolic OH of *α*-T3 by ROS was suggested as mentioned above. The antioxidative activity of Asx-*S*/*α*-T3 (1 : 2)-lipo was higher than additive activity of each single antioxidant liposomes (Fig. 5). As shown in Fig. 8, electronic condition of Asx polyene moiety, which can react with ROS, was affected by intermolecular interaction with *α*-T3 triene chain. Based on these results, it was suggested that contribution of Asx polyene moiety is more dominant than *α*-T3 phenolic hydroxyl group in antioxidative activity of Asx-*S*/*α*-T3 complex.

Asx-*S* is known to be produced specifically by the algae *Haematococcus pluvialis* and the petals of *Adonis annua*,[18] and demonstrated superiority to Asx-*R* and Asx-*meso* in this study. Perhaps the predominance of the Asx-*S* isomer in nature, *e.g.*, in algae *Haematococcus pluvialis*, the petals of *Adonis annua* and *Paracoccus carotinifaciens*,[18,19] might have some additional meaning and significance, similar to vitamins and amino acids.

Based on the findings in this study, compounds that can interact with Asx at the terminal ring moiety and the polyene moiety, might enhance the antioxidative activity of Asx. Such compounds could also be useful as enhancers of Asx functionality. Identification of such enhancer compounds should be the subject of future studies.

In conclusion, we found that the stereochemistry of Asx is an important factor for the induction of the higher antioxidative activity of the liposomes co-encapsulating Asx/*α*-T3 than additive activity of each single antioxidant liposome, with the optimal Asx-*S*/*α*-T3 ratio in liposomes determined to be 1 : 2. Furthermore, the change in the electronic structure of the polyene moiety upon complexation of Asx with *α*-T3, and not the reactivity of the terminal ring moiety, was suggested to be crucial for the potent antioxidative activity of Asx/T3 co-encapsulated liposomes.

Acknowledgment This work was supported by a research program for the development of an intelligent Tokushima artificial exosome (iTEX) from Tokushima University.

Conflict of Interest K. Kogure received a research Grant from Fuji Chemical Industries, Co., Ltd.

References

1) Boussiba S., Fan L., Vonshak A., *Methods Enzymol.*, **213**, 386–391 (1992).
2) Maoka T., *Mar. Drugs*, **9**, 278–293 (2011).
3) Fukuzawa K., *Methods Enzymol.*, **319**, 101–110 (2000).
4) Terao J., *Lipids*, **24**, 659–661 (1989).
5) Lim B. P., Nagao A., Terao J., Tanaka K., Suzuki T., Takama K., *Biochim. Biophys. Acta*, **1126**, 178–184 (1992).
6) Palozza P., Krinsky N. I., *Arch. Biochem. Biophys.*, **297**, 291–295 (1992).
7) Goto S., Kogure K., Abe K., Kimata Y., Kitahama K., Yamashita E., Terada H., *Biochim. Biophys. Acta*, **1512**, 251–258 (2001).
8) Stahl W., Sies H., *Biochim. Biophys. Acta*, **1740**, 101–107 (2005).
9) Hama S., Uenishi S., Yamada A., Ohgita T., Tsuchiya H., Yamashita E., Kogure K., *Biol. Pharm. Bull.*, **35**, 2238–2242 (2012).
10) Hama S., Takahashi K., Inai Y., Shiota K., Sakamoto R., Yamada A., Tsuchiya H., Kanamura K., Yamashita E., Kogure K., *J. Pharm. Sci.*, **101**, 2909–2916 (2012).
11) Kamezaki C., Nakashima A., Yamada A., Uenishi S., Ishibashi H., Shibuya N., Hama S., Hosoi S., Yamashita E., Kogure K., *J. Clin. Biochem. Nutr.*, **59**, 100–106 (2016).
12) Kajimoto K., Yamamoto M., Watanabe M., Kigasawa K., Kanamura K., Harashima H., Kogure K., *Int. J. Pharm.*, **403**, 57–65 (2011).
13) Price M., Reiners J. J., Santiago A. M., Kessel D., *Photochem. Photobiol.*, **85**, 1177–1181 (2009).
14) Jomova K., Valko M., *Toxicology*, **283**, 65–87 (2011).
15) Frisch M. J., Trucks G. W., Schlegel H. B., Scuseria G. E., Robb M. A., Cheeseman J. R., Scalmani G., Barone V., Mennucci B., Petersson G. A., Nakatsuji H., Caricato M., Li X., Hratchian H. P., Izmaylov A. F., Bloino J., Zheng G., Sonnenberg J. L., Hada M., Ehara M., Toyota K., Fukuda R., Hasegawa J., Ishida M., Nakajima T., Honda Y., Kitao O., Nakai H., Vreven T., Montgomery J. A. Jr., Peralta J. E., Ogliaro F., Bearpark M., Heyd J. J., Brothers E., Kudin K. N., Staroverov V. N., Kobayashi R., Normand J., Raghavachari K., Rendell A., Burant J. C., Iyengar S. S., Tomasi J., Cossi M., Rega N., Millam J. M., Klene M., Knox J. E., Cross J. B., Bakken V., Adamo C., Jaramillo J., Gomperts R., Stratmann R. E., Yazyev O., Austin A. J., Cammi R., Pomelli C., Ochterski J. W., Martin R. L., Morokuma K., Zakrzewski V. G., Voth G. A., Salvador P., Dannenberg J. J., Dapprich S., Daniels A. D., Farkas Ö., Foresman J. B., Ortiz J. V., Cioslowski J., Fox D. J., Gaussian 09, Revision D.01; Gaussian, Inc.: Wallingford, CT (2009).
16) Grimme S., Ehrlich S., Goerigk L. J., *J. Comput. Chem.*, **32**, 1456–1465 (2011).
17) Reed A. E., Curtiss L. A., Weinhold F., *Chem. Rev.*, **88**, 899–926 (1988).
18) Jackson H., Braun C. L., Ernst H., *Am. J. Cardiol.*, **101**(10A), 50D–57D (2008).
19) Katsumata T., Ishibashi T., Kyle D., *Toxicol. Rev.*, **1**, 582–588 (2014).